Electronic Supplementary Information

Modulating the Schottky barriers of metal-2D perovskite junctions through molecular engineering of spacer ligands

Zhuo Xu[1*], Weidong Luo[1], Songyan Guo[1], and Shengzhong Frank Liu[1,2,3*]

1 Key Laboratory of Applied Surface and Colloid Chemistry, National Ministry of Education; Shaanxi Key Laboratory for Advanced Energy Devices; Shaanxi Engineering Lab for Advanced Energy Technology; Institute for Advanced Energy Materials; School of Materials Science and Engineering, Shaanxi Normal University, Xi'an 710119, China.

2 Dalian National Laboratory for Clean Energy; Dalian Institute of Chemical Physics, Chinese Academy of Sciences, Dalian 116023, China.

3 University of the Chinese Academy of Sciences, Beijing 100039, China.

Corresponding Authors: * E-mail: xuzh@snnu.edu.cn (X. Z.); szliu@dicp.ac.cn (S. Z. L)

Methods

In this work, the density-functional theory (DFT) calculations were performed using the Vienna Ab initio Simulation Package (VASP). The projected augmented wave (PAW) method and the PBEsol functional within the generalized gradient approximation (GGA) were employed to describe the interaction between ion-cores and valence electrons and the exchange-correlation effects, and an energy cutoff of 500 eV was set for the plane-wave function's expansion. The van der Waals (vdW) dispersion correction was found necessary to yield more accurate lattice constants, which are described by the DFT-D3 correction. The bulk $(HOOCCH_2CH_2CH_2NH_3)_2PbI_4$, $(ClCH_2CH_2NH_3)_2PbI_4$, $(BrCH_2CH_2NH_3)_2PbI_4$, and $(ICH_2CH_2NH_3)_2PbI_4$ structures are optimized by applying Monkhorst-Pack sampling with a Γ-centered 3×3×1, 5×3×1, 5×3×1, and 3×3×2 k-point grid, respectively. The monolayer structures are then cleaved from the optimized bulk structures. The lattice parameters and atomic positions of all the structures were relaxed until the total energy changes were less than 1.0×10^{-5} eV and the maximum force component acting on each atom was less than 0.01 eV $Å^{-1}$. For the contact simulation, in order to form better interfacial lattice matching and minimize the interfacial stress, 2×2×1, 2√2×√2×1, 2√2×√2×1, and 2×2×1 supercell of $(HOOCCH_2CH_2CH_2NH_3)_2PbI_4$, $(ClCH_2CH_2NH_3)_2PbI_4$, $(BrCH_2CH_2NH_3)_2PbI_4$, and $(ICH_2CH_2NH_3)_2PbI_4$ are used to match with the 3√2×3√2×1 metal[001] slabs, a total thickness of seven layer metal atoms is used for the slab model. Periodic boundary condition is applied along the in-plane direction, and a vacuum spacing >20 Å is set along the direction perpendicular to the interface to avoid the interaction between periodic cells in the c direction. Only Gama point sampling is used slab simulations because of the large size of the systems. The bottom four layer metal atoms are fixed during the structure optimization, while the top three layer metal atoms and 2D perovskites are relaxed. The optimization criterion for total energy and maximum force component acting on each atom are 1.0×10^{-5} eV and 0.02 eV $Å^{-1}$ for contact simulations, respectively. The work function and vacuum level are obtained from the calculation of the electrostatic potential across the interfaces.

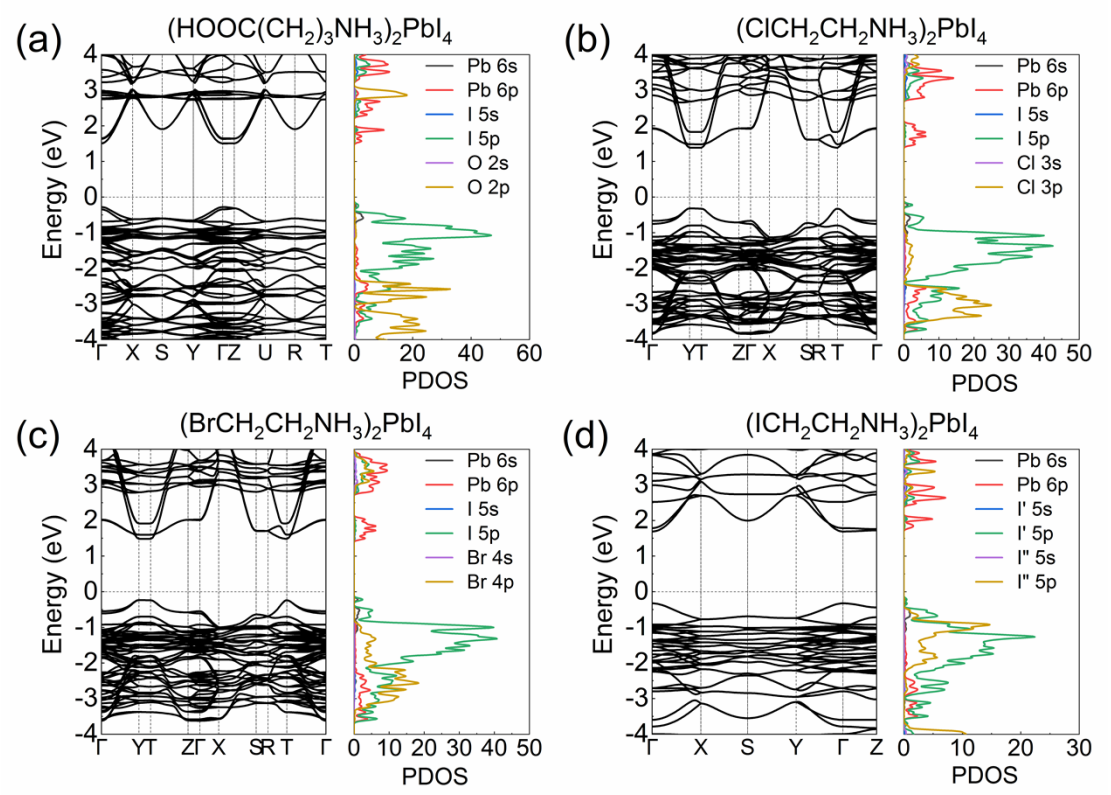

Fig. S1 Band structures and projected density of states (PDOS) for (a) $(HOOCCH_2CH_2CH_2NH_3)_2PbI_4$, (b) $(ClCH_2CH_2NH_3)_2PbI_4$, (c) $(BrCH_2CH_2NH_3)_2PbI_4$, and (d) $(ICH_2CH_2NH_3)_2PbI_4$.

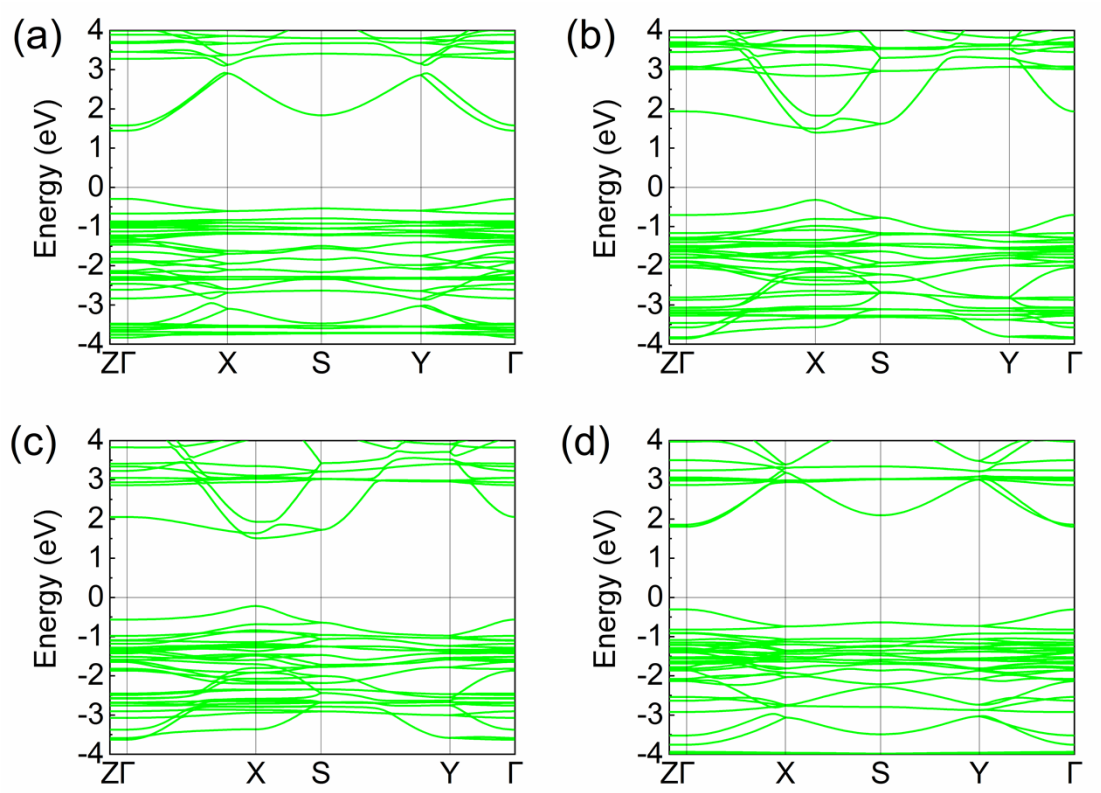

Fig. S2 Band structures for monolayer (a) $(HOOCCH_2CH_2CH_2NH_3)_2PbI_4$, (b) $(ClCH_2CH_2NH_3)_2PbI_4$, (c) $(BrCH_2CH_2NH_3)_2PbI_4$, and (d) $(ICH_2CH_2NH_3)_2PbI_4$.

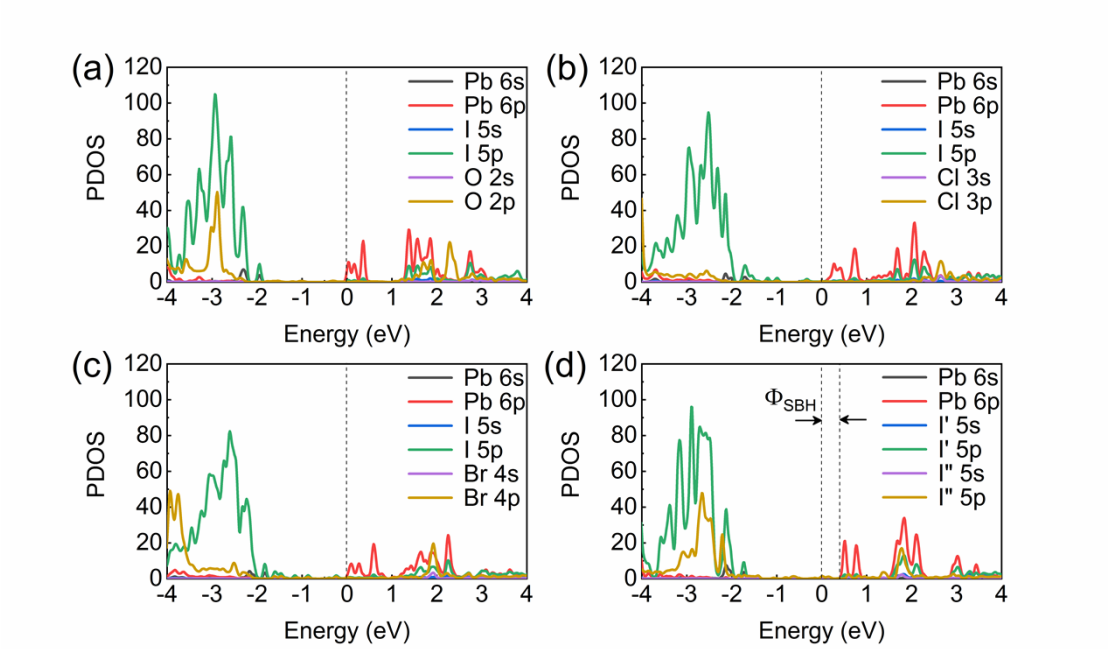

Fig. S3 Projected density of states of Ag– (a) $(HOOCCH_2CH_2CH_2NH_3)_2PbI_4$, (b) –$(ClCH_2CH_2NH_3)_2PbI_4$, (c) –$(BrCH_2CH_2NH_3)_2PbI_4$, and (d) –$(ICH_2CH_2NH_3)_2PbI_4$.

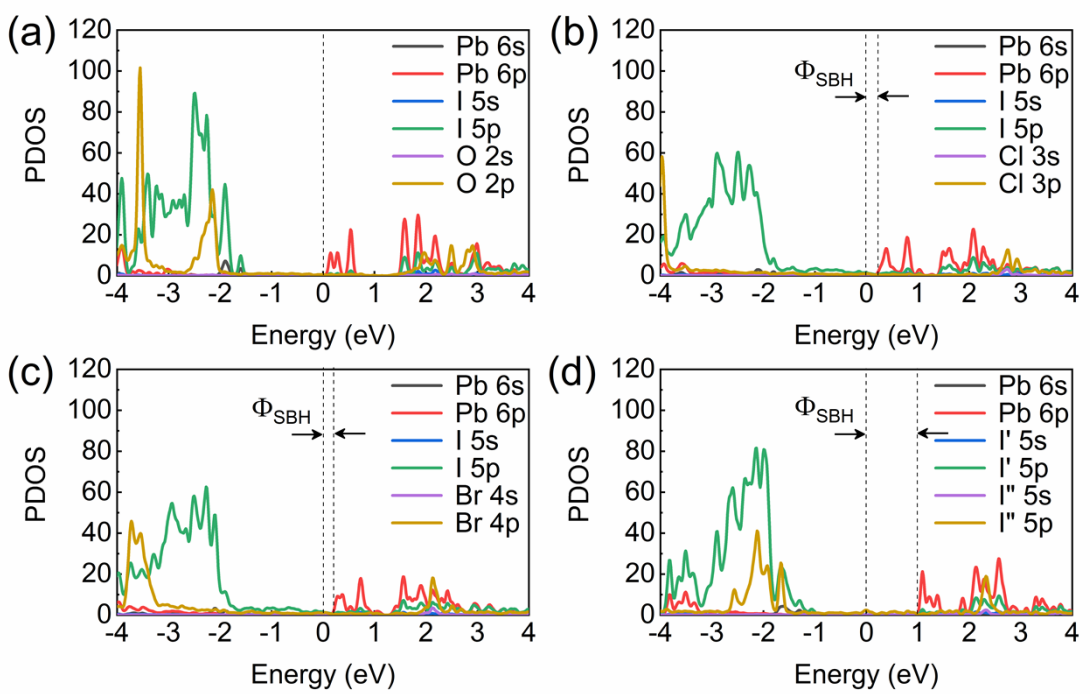

Fig. S4 Projected density of states of Pt– (a) $(HOOCCH_2CH_2CH_2NH_3)_2PbI_4$, (b) – $(ClCH_2CH_2NH_3)_2PbI_4$, (c) –$(BrCH_2CH_2NH_3)_2PbI_4$, and (d) –$(ICH_2CH_2NH_3)_2PbI_4$.

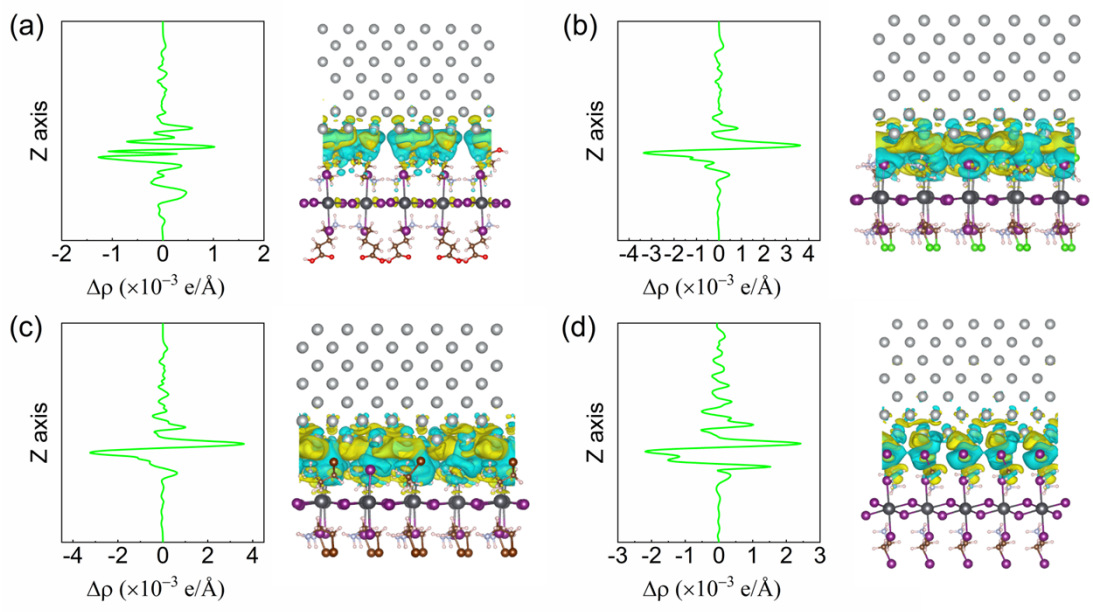

Fig. S5 The charge density difference (Δρ) at the interface region (right-hand panels) and the plane-averaged electron density difference Δρz along the direction perpendicular to the interface (left-hand panels) for Ag– (a) $(HOOCCH_2CH_2CH_2NH_3)_2PbI_4$, (b) $–(ClCH_2CH_2NH_3)_2PbI_4$, (c) $–(BrCH_2CH_2NH_3)_2PbI_4$, and (d) $–(ICH_2CH_2NH_3)_2PbI_4$.

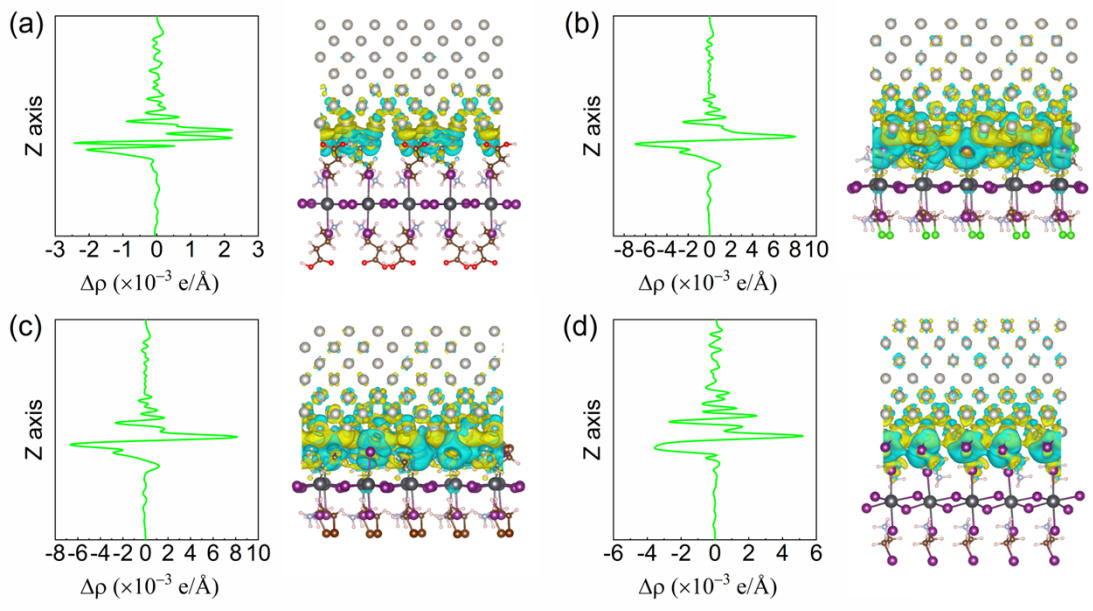

Fig. S6 The charge density difference (Δρ) at the interface region (right-hand panels) and the plane-averaged electron density difference Δρz along the direction perpendicular to the interface (left-hand panels) for Pt– (a) $(HOOCCH_2CH_2CH_2NH_3)_2PbI_4$, (b) $–(ClCH_2CH_2NH_3)_2PbI_4$, (c) $–(BrCH_2CH_2NH_3)_2PbI_4$, and (d) $–(ICH_2CH_2NH_3)_2PbI_4$.

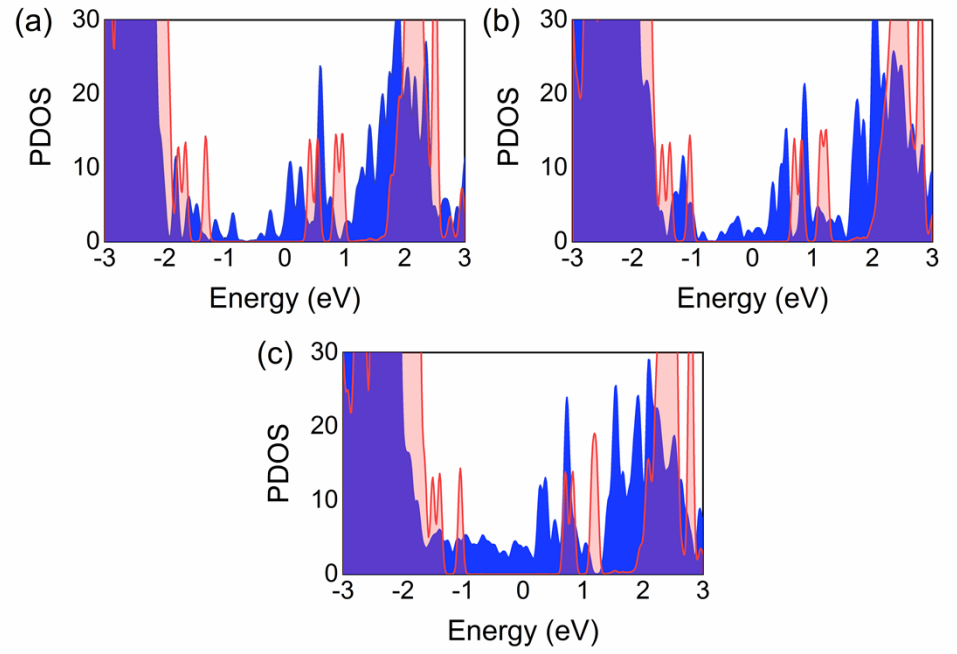

Fig. S7 The red and the blue shaded areas indicate the total DOS projected on the first and the second 2D perovskite layers in (a) Ag–, (b) Au–, and (c) Pt–bilayer $(BrCH_2CH_2NH_3)_2PbI_4$ contact.

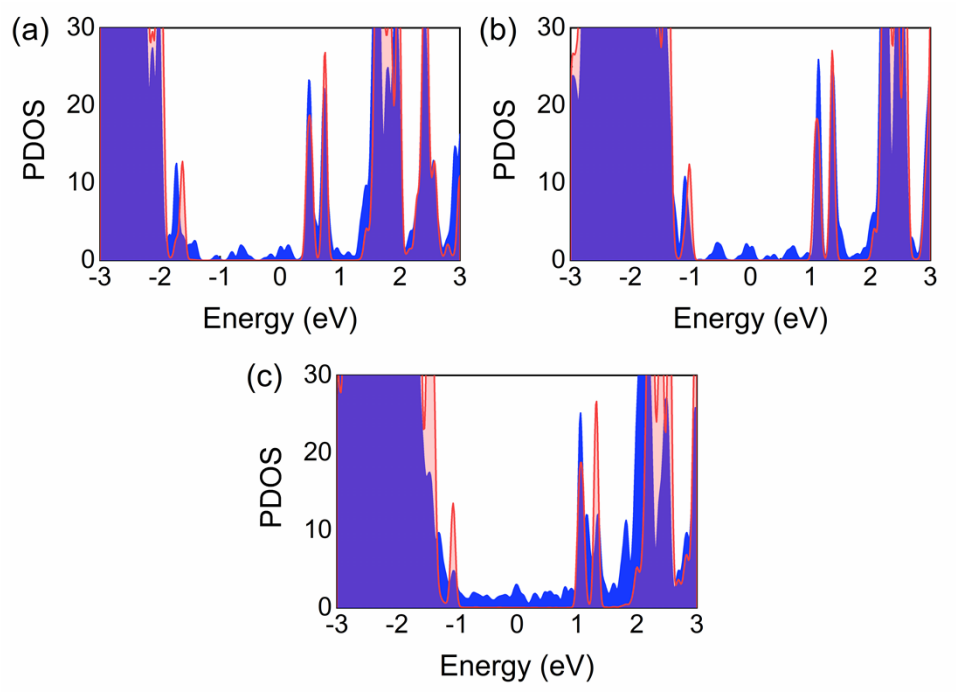

Fig. S8 The red and the blue shaded areas indicate the total DOS projected on the first and the second 2D perovskite layers in (a) Ag–, (b) Au–, and (c) Pt–bilayer $(ICH_2CH_2NH_3)_2PbI_4$ contact.

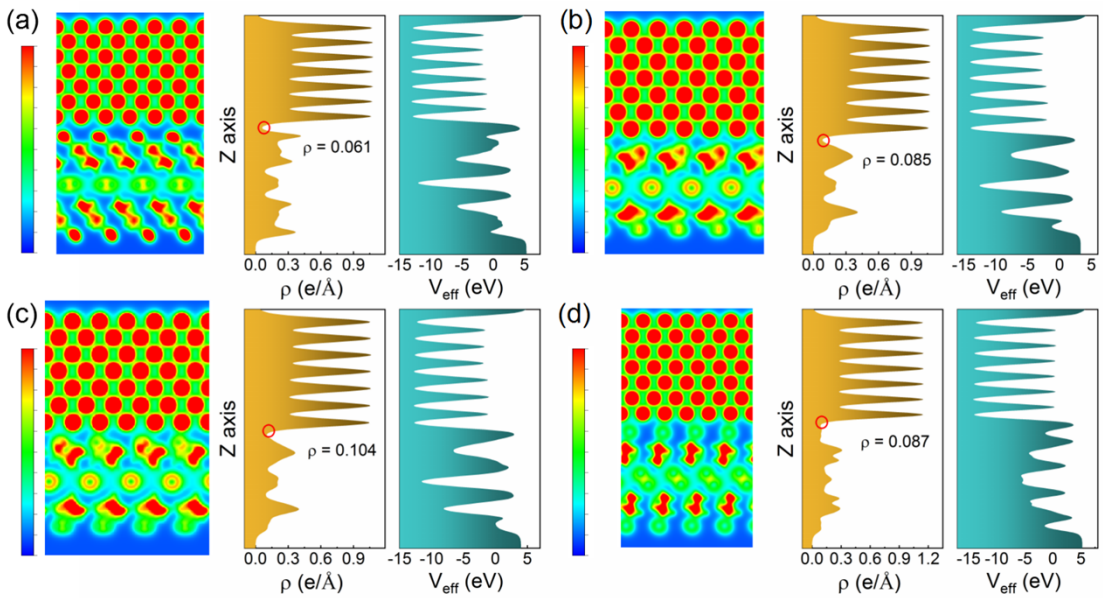

Fig. S9 Average electron densities along x direction projected on the *y*–*z* plane (left panel), average electron density values (ρ) in the *x*–*y* planes normal to the *z* axis (middle panel), and effective potential profiles (right panel) of Ag (a) –$(HOOCCH_2CH_2CH_2NH_3)_2PbI_4$, (b) –$(ClCH_2CH_2NH_3)_2PbI_4$, (c) –$(BrCH_2CH_2NH_3)_2PbI_4$, and (d) –$(ICH_2CH_2NH_3)_2PbI_4$.

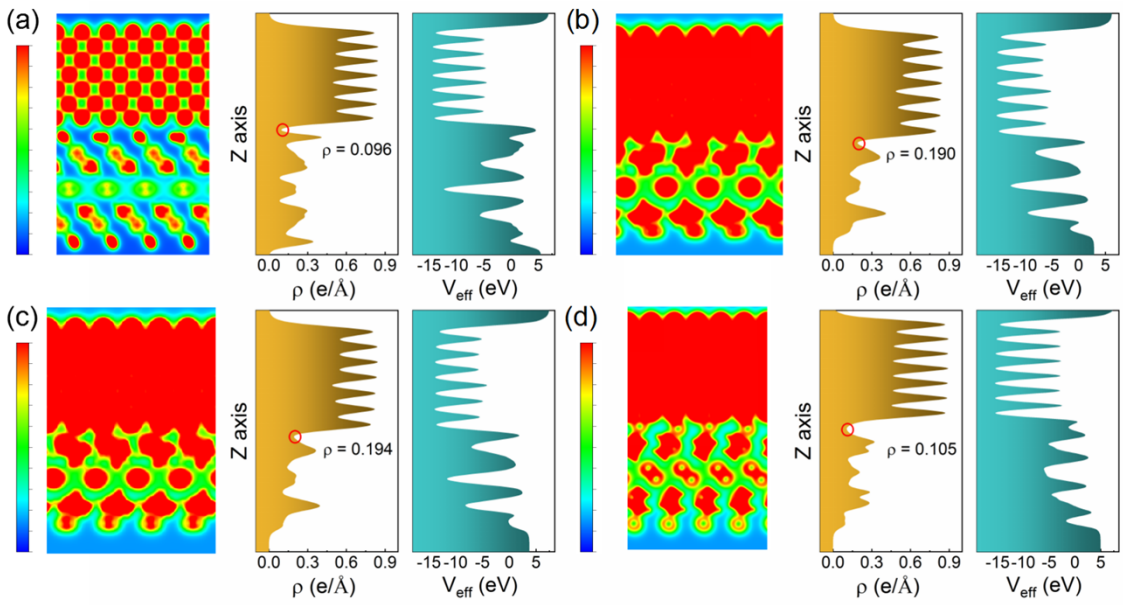

Fig. S10 Average electron densities along x direction projected on the *y*–*z* plane (left panel), average electron density values (ρ) in the *x*–*y* planes normal to the *z* axis (middle panel), and effective potential profiles (right panel) of Pt (a) –$(HOOCCH_2CH_2CH_2NH_3)_2PbI_4$, (b) –$(ClCH_2CH_2NH_3)_2PbI_4$, (c) –$(BrCH_2CH_2NH_3)_2PbI_4$, and (d) –$(ICH_2CH_2NH_3)_2PbI_4$.